

1 **Appendix A: Supplementary material**

2 **Model and setup**

3 The chemistry package in WRF-Chem consists of the following main components; a dry
4 deposition scheme, anthropogenic emissions, biogenic emission, gas-phase chemical
5 mechanisms, photolysis schemes and aerosol schemes. The choices for the physical
6 parameterization are based on available literature, in additions to tests executed for the
7 purpose of this study (not shown). Tests include the choices of planetary boundary layer
8 (PBL) schemes, chemical initial and boundary conditions, horizontal and vertical resolution,
9 in addition to several choices for nudging parameters.

10 The OsloCTM3 simulation was driven by meteorological data from the ECMWF-IFS model
11 and run with ECLIPSE version 5 anthropogenic emissions (Stohl et al., 2015), GFED version
12 3 monthly biomass burning emissions (Randerson et al., 2013; van der Werf et al., 2006) and
13 year 2000 MEGAN version 2.1 natural emissions (Guenther et al., 2006b).

14 The TNO dataset is a gridded emissions inventory covering UNECE-Europe for the years
15 2003-2009. It contains European air pollutant emissions (CH_4 , CO , NH_3 , NMVOC, NO_x ,
16 PM_{10} , $\text{PM}_{2.5}$ and SO_2) per source sector, and the emissions from area sources have been
17 distributed in a sector-specific way, while the point source emissions keep their particular
18 coordinates (Denier van der Gon et al., 2010a; Denier van der Gon et al., 2010b). For the
19 measurement period in 2002, anthropogenic emissions from 2003 had to be used.

20 For the biogenic emissions, the MEGAN (Model of Emissions of Gases and Aerosols from
21 Nature) emissions inventory (Guenther et al., 2006) and the pre-processor are used.

22 **Measurements**

23 The concentration and the flux are derived directly from measurements, giving the value for
24 the total resistance. The aerodynamic resistance is derived in the model using Monin-
25 Obukhov similarity theory, and the sub-laminar resistance is calculated using
26 parameterization by Hicks et al. (1987). The surface resistance is given as a residual based on
27 values of the other variables. The surface resistance is divided in two; stomatal and non-
28 stomatal resistance, which are placed in parallel.

1 Ozone, water and energy fluxes were measured by the eddy covariance technique, and the
2 partitioning of fluxes in to stomatal and non-stomatal ozone flux was estimated utilizing a Dry
3 Depositions Inferential Method (DDIM) based on a big leaf assumption. The stomatal
4 resistance is calculated by inverting the Penman-Monteith equation (Monteith 1981; Gerosa et
5 al. 2005) and solving it for the water vapor resistance, which is scaled by the ratio of the
6 diffusivity of ozone in air to that of water vapor, giving an expression for the stomatal
7 resistance, and hence the stomatal conductance, of ozone. When the stomatal resistance is
8 known the non-stomatal one can be found as a residual. Further details of the Penman-
9 Monteith equation and estimation of the stomatal flux from measurements are found in
10 Gerosa et al. (2005).

11 Several conditions had to be fulfilled for the data screening process, among them stationarity
12 requirements according to (Dutaur et al., 1999), and capturing efficiency. Further detail about
13 the data screening process is found in the respective publications for each measurement
14 campaign.

15 Measurements for the maquis ecosystem were made a few kilometers from the holm oak
16 measurement site. At the site 90% of the vegetation consists of 6 species (*Quercus ilex*,
17 *Arbutus unedo*, *Rosmarinus officinalis*, *Cistus spl*, *Phyllirea latifolia* and *Erica multiflora*),
18 composing a typical Mediterranean maquis ecosystem, with an average height of 120 cm. The
19 full measurement period and site of measurements have been described in more detail in cited
20 publications (Table 2). The evergreen broadleaf forest was represented by vegetation in a
21 second area, characterized by the dominance of holm oak (*Quercus ilex* L.) with an average
22 height of about 12-13 m. Due to its coastal location land sea-breeze is pronounced during
23 summer (Gerosa et al., 2009b). In contrast to the previous year, the 2004 summer was colder
24 and wetter, and more representative for average meteorological conditions at this site.

25 Measurements in the barley field were selected from a field campaign during the spring and
26 summer periods of 2002. The total measurement period was April 3-July 17, and the selected
27 sub-period is representative of the barley's anthesis, in May 10-22, which represents the
28 period with the highest measured ozone fluxes (Gerosa et al., 2004). More details about the
29 measurement site and period is found in Gerosa et al. (2004).

30 Measurements of the relative maximum stomatal conductance and hourly accumulated VPD
31 for the pooled data over all measurement periods for the holm oak forest is used to derived a
32 critical VPD limit of 20 kPa h, and is shown in Fig. A4.

1 **Ozone mixing ratios and meteorological conditions**

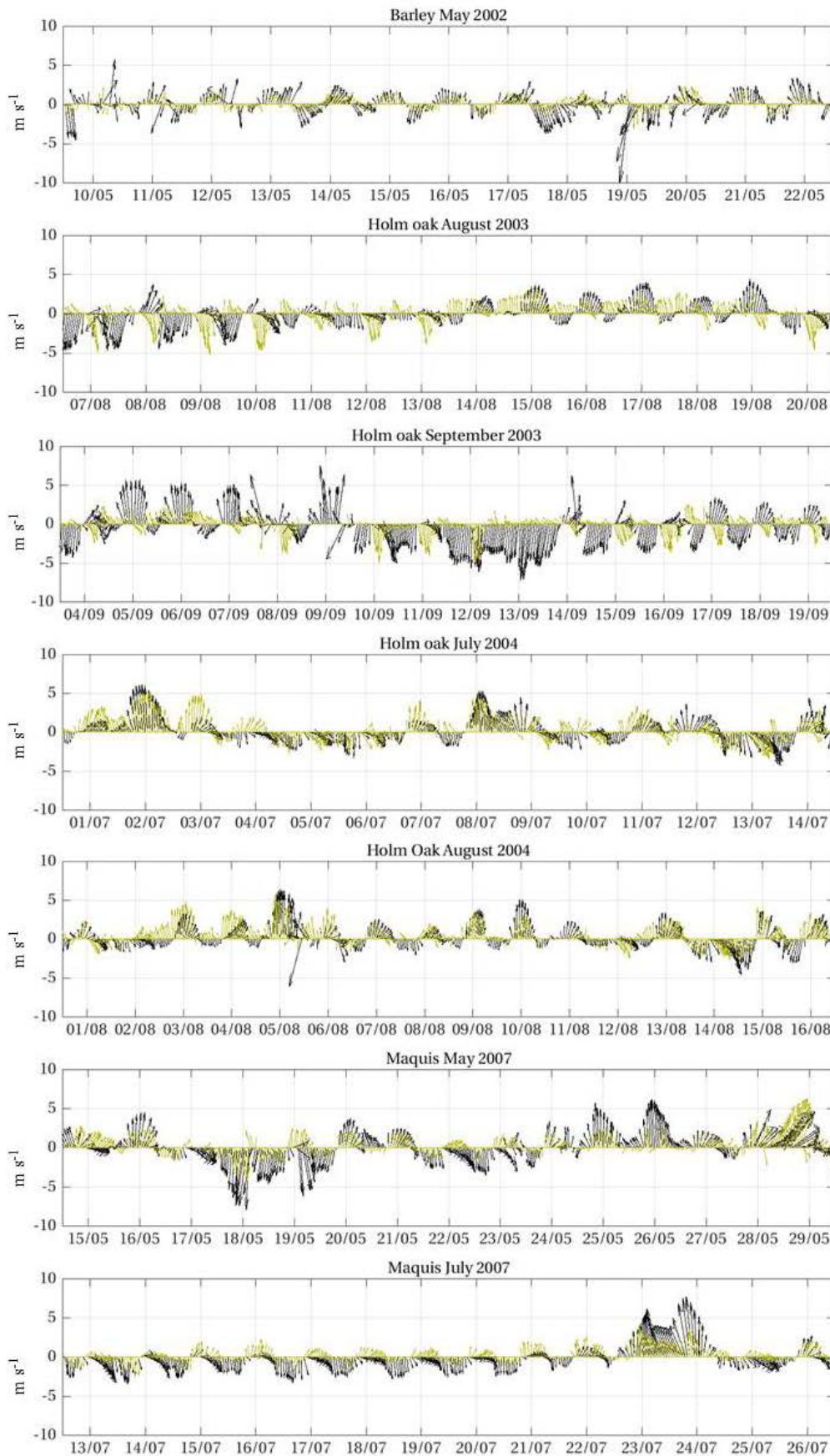
2 For the Maquis ecosystem, the model somewhat underestimates the midday peak
3 temperatures on some days during the May period, which coincide with high wind (Fig. A1)
4 and thick PBL situations. This affects the ozone mixing ratios, which are underestimated
5 during the daytime. Also, some night values are somewhat overestimated as compared to
6 measurements. For the July period, both the measured and modelled mean temperature over
7 the period is 24°C, and the model reproduces the temperature variations well. The wind
8 speeds are low in both measurements and model throughout the period (Fig. A1), however the
9 consistent land-sea breeze evident from the measurements for most of the period is
10 recognizable in the model grid cell output. Underestimation of modelled nighttime values of
11 ozone mixing ratios leads to an overall underestimation of the average values for the period of
12 39 ppb as compared to the measured value of 43 ppb.

13 For the Barley field, the model overestimate the average wind speed, which is on average 2.7
14 m s^{-1} , compared to the measured wind which is on average 1.2 m s^{-1} for the period. The
15 average measured ozone mixing ratio for the period is 34.7 ppb and the same for the model.
16 The exact match hides the fact that although the diurnal variation is well represented on most
17 days, the nighttime values are overestimated by the model, and the peak midday values are
18 underestimated. This underestimation is most likely linked to the meteorological conditions,
19 with too high modelled wind speeds (Fig. A1), and underestimated midday temperatures for
20 the same days (Fig. 2).

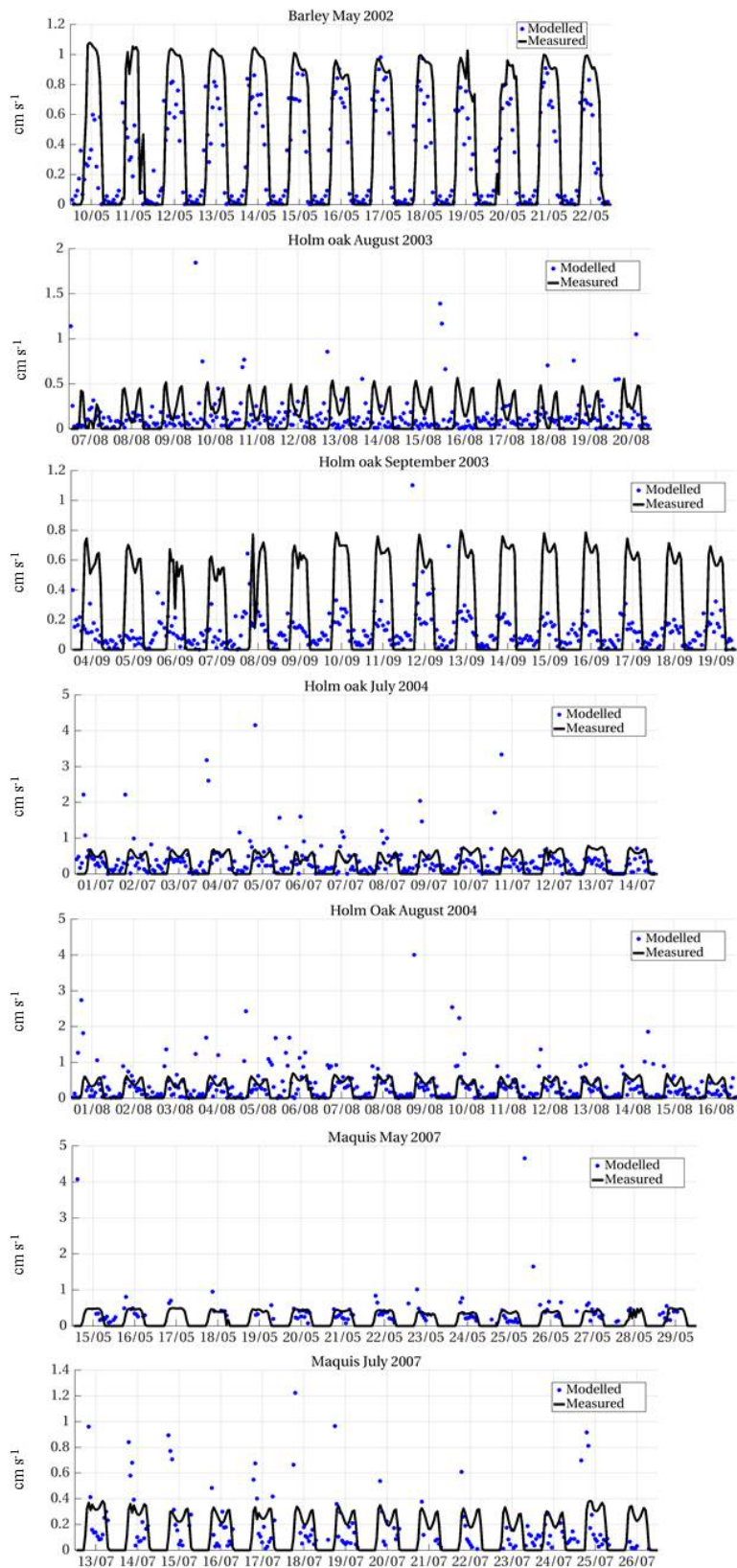
21 The 2003 September period was not as warm as the August period and temperatures are much
22 better represented by the model during this period. The wind pattern for the period is not as
23 well captured, and the winds are stronger in both model and measurements in this period (Fig.
24 A1). As a result, the ozone mixing ratios during midday are underestimated by the model
25 throughout the period. The nighttime values are often overestimated, and the timing for the
26 low values in the early morning hours is shifted as compared to the measurements.

27 The results for 2004 are regarded to be closer to the normal meteorological and chemical
28 conditions for the site and more representative for this type of vegetation. The ozone mixing
29 ratios during the period is somewhat underestimated during daytime and underestimated
30 during night as compared to the measurements. The 2004 August period is slightly warmer
31 compared to the July period of the same year. Daytime values for the period are well

1 estimated by the model. However; the nighttime values are overestimated throughout the
2 period, especially in the early morning hours.



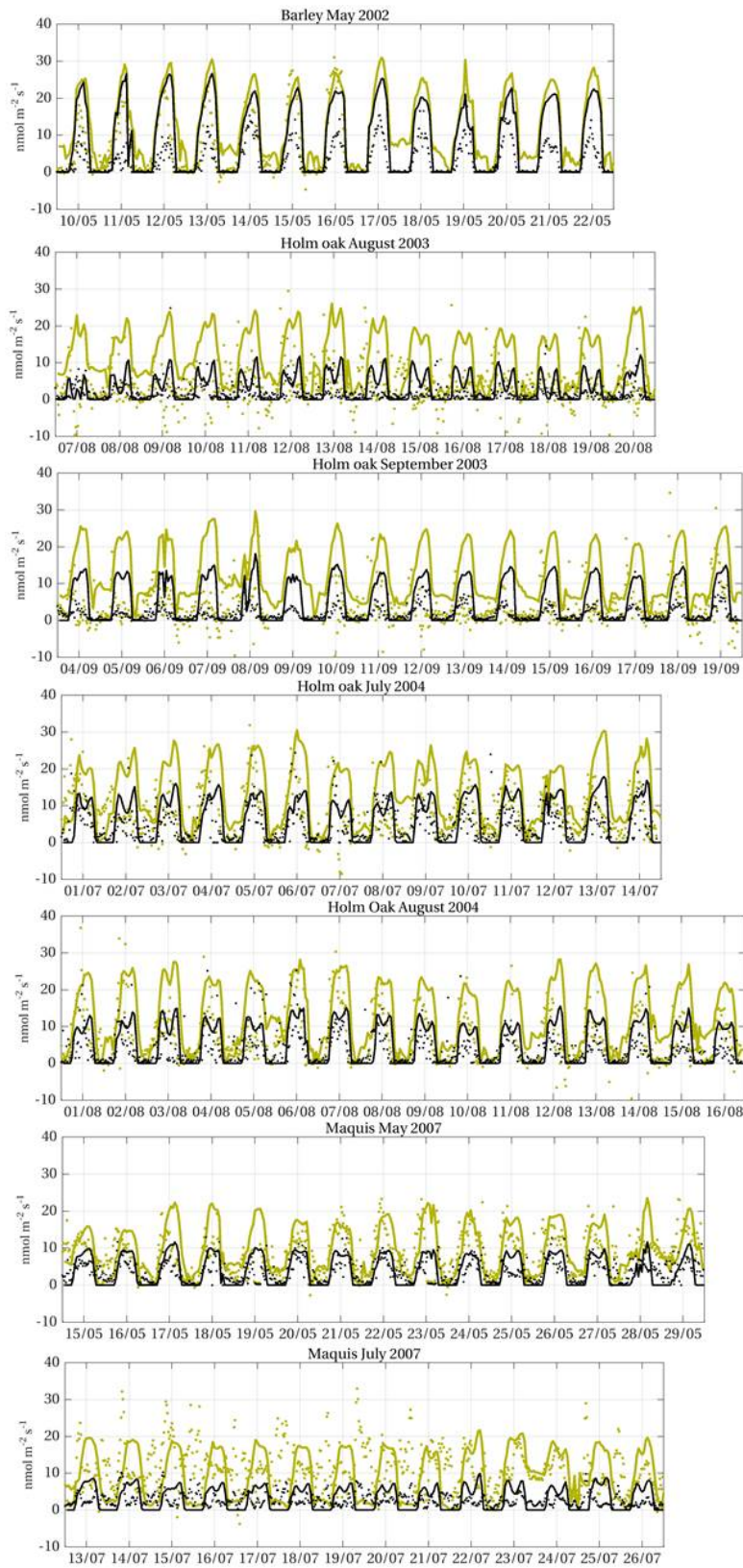
$\frac{1}{2}$ A1: Modelled (black) and measured (green) wind for each measurement period.



1
2

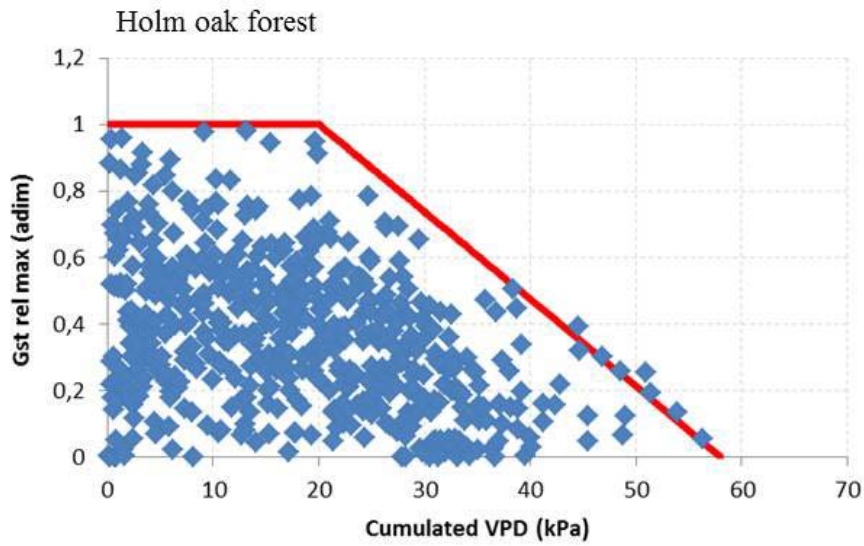
3 Figure A2: Measured (dots) and modelled (lines) stomatal conductance for each measurement period.

4 Note the differences in scale between panels.



1
2

3 Figure A3: Measured (dots) and modelled (lines) total (green) and stomatal (black) ozone fluxes for
4 each measurement period. Note the differences in scale between panels.



1

2 Figure A4. Pooled data for all measurement periods for the relative maximum stomatal conductance
3 and hourly accumulated VPD, forming the basis for the estimated critical VPD value of 20 kPa h for
4 the holm oak forest.